Impact of Annealing on the Relaxation Processes in Pt/$SrTiO_3$/Pt Thin Film Capacitors

H. Ouajji[a,b,*], K. Raouadi[b], B. Yangui[b] and J. Guillan[c]

[a]Grenoble Electrical Engineering Laboratory (G2ELab), University of Grenoble, 25 Rue des Martyrs, BP 166, 38042 Grenoble Cedex 9, France

[b]Laboratory for Materials, Organization and Properties (LMOP), University of Tunis El Manar, Campus Universitaire-El Manar, 2092 Tunis, Tunisia

[c]STMicroelectronics, 38926 Crolles Cedex, France

(Received June 5, 2011; in final form March 8, 2016)

In this paper, the effect of the post-annealing on the dielectric properties of $SrTiO_3$ thin films (200 nm) grown by ion beam sputtering has been investigated. The measured dielectric constant dramatically increased after the post-annealing which is a consequence of the formation of the perovskite phase. A low frequency relaxation mechanism is clearly identified in the amorphous state of this material. Once crystallized, a second relaxation mechanism of lower amplitude is detected at high frequencies and for high measuring temperature. It is assumed that this second relaxation process is related to the space charges bound at the grain boundaries, whereas the first one was assigned to the thermally activated motions of the ionized oxygen vacancies and interfacial polarization under alternating field.

DOI: 10.12693/APhysPolA.130.791

PACS/topics: 84.32.Tt, 84.37.+q, 81.15.Cd, 73.61.–r, 77.22.Gm, 76.60.Es

1. Introduction

The high permittivity of strontium titanate ($SrTiO_3$) thin layers makes these materials attractive as integrated capacitors for microelectronics. However, ferroelectrics with a high permittivity can only be obtained for the crystalline phase which usually requires high annealing temperatures (> 600 °C). Such layers can be grown on various substrates by several deposition techniques such as: pulse laser deposition (PLD) [1–4], metal-organic chemical vapor deposition (MOCVD) [5], radio-frequency magnetron sputtering [6–9] and ion beam sputtering (IBS) [10, 11]. Most of these processes are generally performed and prepared at deposit temperatures higher than 400 °C in order to obtain high-quality crystalline layers necessary to achieve high dielectric constants greater than 100. However, for some applications it is interesting to obtain these layers at processing temperatures lower than 400 °C (e.g. concept of above integrated circuit). In the present research, $SrTiO_3$ films were deposited using the IBS method, which is a relatively low temperature technique. In this case, a post-annealing is necessary to obtain a high permittivity. Compared with radio-frequency magnetron sputtering method, the IBS method is considered to be more advantageous in term of the flexibility of the deposition condition and of reduced plasma damage of the film. In this work, we studied the effect of annealing on the dielectric constant ε' and dielectric loss ($\tan\delta$) of $SrTiO_3$ thin films within large frequency and temperature ranges. This study deals with the dielectric behavior of the amorphous and/or crystalline phase, as revealed by a real change of the dielectric constant. Furthermore, it is pointed out that a better understanding of the loss mechanisms at low frequencies will contribute to improvement of the dielectric properties. A detailed analysis of the dielectric relaxation phenomena is then presented.

*corresponding author; e-mail: ouadjihayet@yahoo.fr

2. Experimental details

$SrTiO_3$ (STO) thin films with a typical thickness of 200 nm were deposited at room temperature by IBS on Pt/TiO_2/SiO_2/Si substrates. Details on the thin films grown process are reported elsewhere [10]. After deposition, the films were submitted to an annealing treatment at different temperatures, ranging from 250 to 550 °C, for 30 min in a conventional furnace in ambient air. To perform the electrical measurements, circular top platinum electrodes with 110 µm in diameter were patterned by photolithography and lift-off process. The dielectric properties (dielectric constant ε', dissipation factor $\tan\delta$) of STO thin films were measured in terms of frequency (0.01 Hz–1 MHz) and measuring temperature (T_{meas}) (30 °C to 200 °C), using an ALPHA high resolution dielectric analyzer (Novocontrol BDS20).

3. Results and discussion

3.1. Impact of annealing on the dielectric constant

The effect of post-deposition annealing temperatures on the structural properties of STO films was studied previously [12]. It was shown that as-deposited films were amorphous (no STO peaks observed) and the crystallization starts to occur at a temperature around 321 °C. This

low temperature crystallization is crucial for above integrated circuits and justifies the choice of STO material for this type of application [13].

Figure 1 show the variation of the dielectric constant with the annealing temperature for frequency equal to 1 MHz and a measurement temperature to 200 °C.

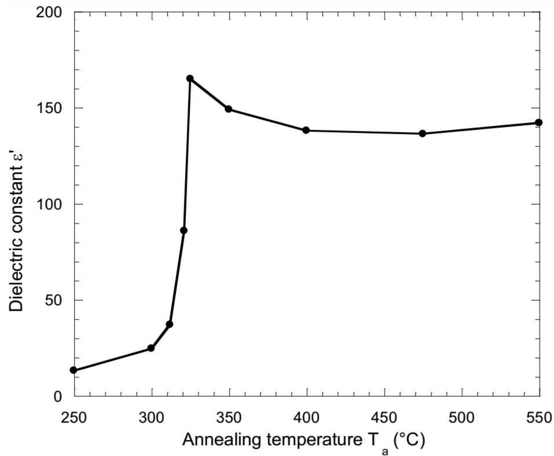

Fig. 1. Dielectric constant versus annealing temperatures (T_a) for frequency equal to 1 MHz and a measurement temperature to 200 °C.

First, the strong increase in ε', as observed when T_a increases from 300 °C to 325 °C is assigned to the amorphous to crystalline transition. This result is consistent with the X-ray diffraction (XRD) analysis already reported [12]. The dielectric constant of the STO film annealed at 325 °C exhibits a peak at a value of 160. Also, an annealing treatment carried out at 400 °C leads to a quasi-stable value of the dielectric constant which is roughly 140. A further increase in annealing temperature results in a slight change of the dielectric constant. To date, the dielectric behavior of the STO thin films in the narrow temperature range corresponding to the amorphous-crystalline transition was not reported so far. Several assumptions can be provided to explain the reduction in ε' for STO films annealed in the range of T_a between 325 °C and 400 °C. According to some reports [14, 15], a decrease in the dielectric constant of the $SrTiO_3$ thin films has been observed when the material thickness decreases, due to the interfacial effects. In our case, the thickness is controlled and its possible variation did not lead to a noticeable change in the dielectric constant value. The dielectric constant is also related to the crystallization as well as the crystal grain size [16]. During the crystallization, a large number of crystalline grains are indeed generated which is responsible for changes in the dielectric constant value. This change is consistent with the observations performed by means of atomic force microscopy carried out on STO films annealed at different temperatures [12].

Furthermore, previously works [17–20] reported that an extension or compressive stress influenced strongly the permittivity value of $SrTiO_3$. A compressive stress in the plan of the layers involves a decrease in ε value [17]. This behavior is rather related to the soft-mode phonon which was the subject of several works dealing with the permittivity value in $SrTiO_3$ compound [21, 22]. This mode comes from the vibration of Ti and O ions and takes part in the atomic polarizability (i.e. ionic) of $SrTiO_3$. A compressive stress hardens the soft-mode phonon which results in a reduced motion of these ions and thus with a permittivity decrease. Intrinsic stress in the material is the principal factor of the decrease in the dielectric constant between 325 °C and 400 °C, since the coexistence of two phases (amorphous and crystalline) cannot be excluded in this temperature range and could induce a compressive stress in the material.

3.2. *Frequency and temperature dependence of the dielectric constant*

Figure 2 depicts the frequency dependence of the dielectric constant ε' for different measuring temperatures T_meas ranging from 30 to 200 °C and two different types of annealed samples (amorphous films, $T_\mathrm{a} = 300$ °C

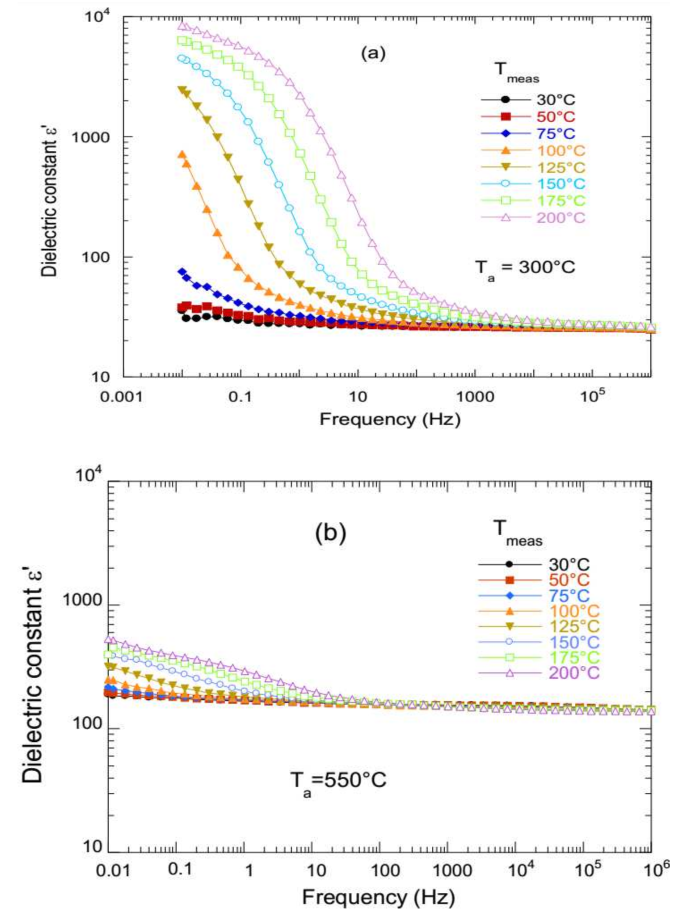

Fig. 2. The frequency dependence of the dielectric constant ε' for different measuring temperatures T_meas ranging from 30 to 200 °C and two different types of annealed samples: (a) amorphous films $T_\mathrm{a} = 300$ °C and (b) polycrystalline films, $T_\mathrm{a} = 550$ °C.

in Fig. 2a and polycrystalline films, $T_a = 550\,°C$ in Fig. 2b). For frequencies higher than 1 kHz, the dielectric constant depends on both frequency and T_a. Moreover, in this figure (Fig. 2a,b) the effect of annealing temperature on the dielectric constant value is clearly demonstrated and can be discussed as follows: (i) the dielectric constant value varies from 25 to 140 when T_a increases from 300 °C to 550 °C. The lower value corresponds to the amorphous state of the film, while the highest one is well associated with the formation of the crystalline phase. (ii) The strong dispersion phenomenon observed at low frequency which may be due to the migration of oxygen vacancies to the interface film/electrode is well reduced for 550 °C as annealed temperature. This implies that the density of defects and interface traps could be much reduced through post-annealing process.

3.3. Impact of annealing on the relaxation processes

Figure 3 shows the frequency response of the dielectric loss ($\tan\delta$) for the frequencies range 0.01 Hz–1 MHz at temperatures ranging in 30–200 °C domain. In the amorphous phase (Fig. 3a), a relaxation peak (labeled "relaxation 1") is clearly evidenced. In the crystalline phase (Fig. 3b), two relaxations peaks were detected. When the measuring temperature decreases, the first relaxation peak is shifted toward low frequencies and the peak magnitude decreased slightly. The second peak (labeled "relaxation 2" in Fig. 3b) presents a weak amplitude and it is detected at high frequency for high measuring temperature. The positions of both relaxation peaks shift apparently toward high frequencies when temperature increases. This phenomenon indicates that these two peaks are associated with a thermally activated relaxation process. On the other hand, Fig. 4a,b depicts the Arrhenius behavior for samples subjected to different annealing temperatures. The activation energy of first relaxation process is extracted from the Arrhenius plot and it is found to be around 1 eV. This value agrees well with those (0.9–1.2 eV) determined for ionic motion of oxygen vacancies in titanate materials [23, 24]. Relaxation 1 (Fig. 4a) may be probably explained by the migration of ionic charges from one electrode to the other and blocking of charges at the metal — $SrTiO_3$ interfaces. The presence of grains slows down this migration inter-electrodes and may explain the shift of this relaxation towards lower frequencies when the material

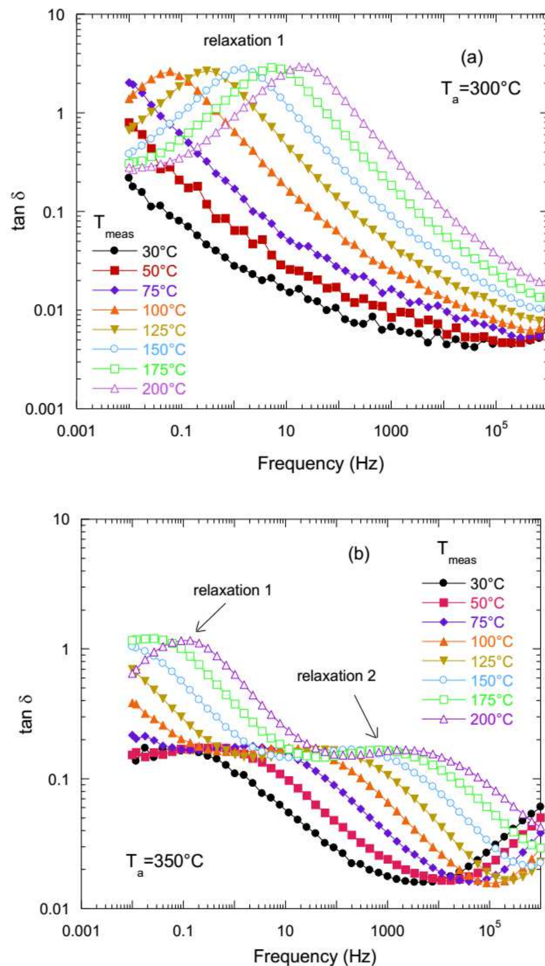

Fig. 3. Frequency response of the dielectric loss for: (a) amorphous films ($T_a = 300\,°C$); (b) polycrystalline films ($T_a = 350\,°C$).

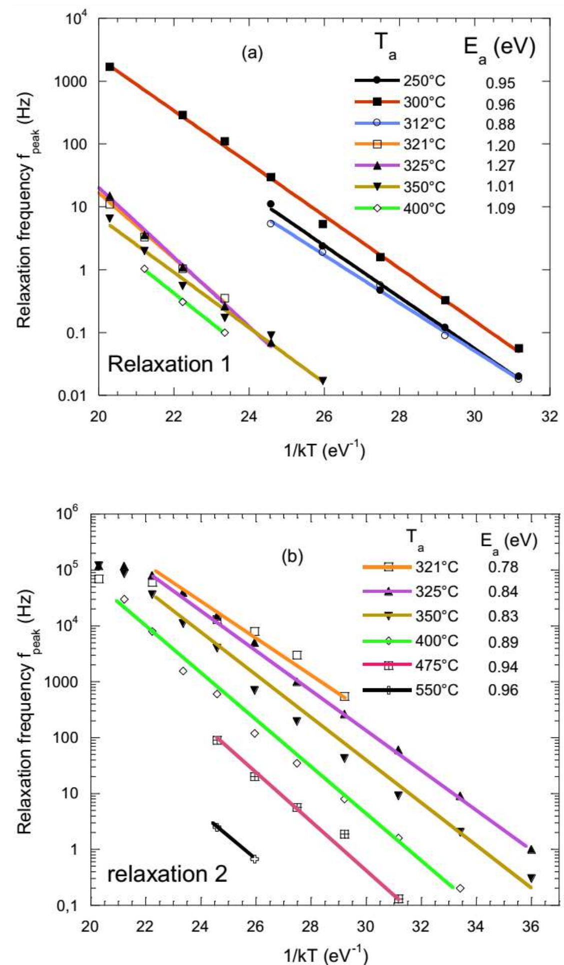

Fig. 4. Arrhenius plot for relaxations 1 and 2.

crystallizes. Once crystallized, a second relaxation mechanism of lower amplitude, is identified at high frequency and temperature as compared to first mechanism. For polycrystalline thin films, the grain boundary effects become crucial and are thought to be one of the main mechanism of loss in dielectric materials, along with defects are associated with oxygen vacancies and polar regions [25]. Local polar regions may be induced by defects, grain boundaries. These latter can be responsible for second relaxation mechanism [25].

4. Conclusion

The annealing effects on the dielectric properties of the STO films deposited by IBS have been carried out. The polycrystallization of STO film improves some electrical properties such as the increase of the dielectric constant. However, the grain boundary effects become crucial and are thought to be one of the main mechanisms of loss in dielectric materials. Consequently, a second relaxation mechanism is obvious in the plot of dielectric loss ($\tan\delta$) versus frequency.

Acknowledgments

This work was carried out as part of an AUF (Agence Universitaire de la Francophonie) exchange program between France and Tunisia. The first author is indebted to AUF for providing financial support during the preparation of his Ph.D. thesis.

References

[1] E.J. Tarsa, E.A. Hachfeld, F.T. Quinlan, J.S. Speck, M. Eddy, *Appl. Phys. Lett.* **68**, 490 (1996).

[2] N. Sugii, K. Takagi, *Thin Solid Films* **323**, 63 (1998).

[3] M. Lippmaa, N. Nakagawa, M. Kawasaki, S. Ohashi, H Koinuma, *J. Electroceram.* **4**, 365 (2000).

[4] C. Ang, L.E. Cross, Z. Yu, R. Guo, A.S. Bhalla, J.H. Hao, *Appl. Phys. Lett.* **78**, 2754 (2001).

[5] H. Yamaguchi, P.-Y. Lesaicherre, T. Sakuma, Y. Miyasaka, A. Ishitani, M. Yoshida, *Jpn. J. Appl. Phys.* **32**, 4069 (1993).

[6] S. He, Y. Li, X. Liu, B. Tao, D. Li, Q. Lu, *Thin Solid Films* **478**, 261 (2005).

[7] S.-H. Nam, H.-G. Kim, *Appl. Phys. Lett.* **72**, 2895 (1992).

[8] K. Matsui, M. Taga, T. Kobayashi, *Jpn. J. Appl. Phys.* **32**, 796 (1993).

[9] A.B. Kozyrev, T.B. Samoilova, A.A. Golovkov, A.M. Prudan, O.I. Soldatenkov, D. Koepf, *J. Appl. Phys.* **84**, 3326 (1998).

[10] J. Guillan, G. Tartavel, E. Defaÿ, L. Ulmer, L. Galéra, B. André, F. Baume, *Integr. Ferroelectr.* **67**, 93 (2004).

[11] H. Yamamichi, T. Sakuma, K. Takemura, Y. Miyasaka, *Jpn. J. Appl. Phys.* **30**, 2193 (1991).

[12] F. Jomni, H. Ouajji, A. Sylvestre, J. Guillan, E. Defaÿ, C. Dubarry, K. Raouadi, B. Yangui, *Integr. Ferroelectr.* **100**, 228 (2008).

[13] E. Defaÿ, D. Wolozan, J.P. Blanc, E. Serret, P. Garrec, S. Verrun, D. Pellissier, P. Delpech, J. Guillan, B. André, L. Ulmer, M. Aïd, P. Ancey, *Solid State Electron.* **51**, 1624 (2007).

[14] B.T. Lee, C.S. Hwang, *Appl. Phys. Lett.* **77**, 124 (2000).

[15] C. Zhou, D.M. Newns, *J. Appl. Phys.* **82**, 3081 (1997).

[16] K.T. Kang, M.H. Lim, H.G. Kim, I.D. Kim, J.M. Hong, *Thin Solid Films* **516**, 1218 (2008).

[17] T. Schimizu, *Solid State Commun.* **102**, 523 (1997).

[18] T.M. Shaw, Z. Suo, M. Huang, E. Liniger, R.B. Laibowitz, J.D. Baniecki, *Appl. Phys. Lett.* **75**, 2129 (1999).

[19] W. Chang, C.M. Gilmore, W.-J. Kim, J.M. Pond, S.W. Kirchoefer, S.B. Qadri, D.B. Chirsey, J.S. Horwitz, *J. Appl. Phys.* **87**, 3044 (2000).

[20] S. Hyun, K. Char, *Appl. Phys. Lett.* **79**, 254 (2001).

[21] T. Ostapchuk, J. Petzelt, V. Zelezny, A. Pashkin, J. Pokorny, I. Drbohlav, R. Kuzel, D. Rafaja, B.P. Gorshunov, M. Dressel, Ch. Ohly, S. Hoffmann-Eifert, R. Waser, *Phys. Rev. B* **66**, 235406 (2002).

[22] J. Petzelt, T. Ostapchuk, A. Pashkin, I. Rychetsky, *J. Europ. Ceram. Soc.* **23**, 2627 (2003).

[23] R. Waser, *J. Am. Ceram. Soc.* **74**, 1934 (1991).

[24] S. Saha, S.B. Krupanidhi, *J. Appl. Phys.* **87**, 849 (2000).

[25] C.V. Weiss, M.W. Cole, S.P. Alpay, E. Ngo, R.C. Toonen, S.G. Hirsch, J.D. Demaree, C. Hubbard, *Integr. Ferroelectr.* **100**, 36 (2008).